ATIPC – 2020 Special Issue

J. Indian Chem. Soc.,
Vol. 97, No. 12b, December 2020, pp. 2805-2813

Exclusion of crystal violet and methylene blue from wastewater using titanate nanotube: Kinetics of the adsorption and photodegradation

Saismrutiranjan Mohanty[a], Sanjib Moulick[b], Shuvendu Singha[a] and Sanjoy Kumar Maji*[a]

[a]Department of Chemistry, School of Applied Sciences, KIIT Deemed to be University, Bhubaneswar-751 024, Odisha, India

[b]School of Civil Engineering, KIIT Deemed to be University, Bhubaneswar-751 024, Odisha, India

E-mail: maji.sanjoy@gmail.com

Manuscript received online 09 December 2020, accepted 28 December 2020

Photo-adsorption of crystal violet (CV) and methylene blue (MB) from synthetic wastewater using hydrothermally synthesized titanate nanotubes (TNTs), a cheap adsorbent/photocatalyst was reported. Experimental results suggested 3 g/L dose of TNTs could efficiently adsorb/degrade CV (initial concentration: 20 mg/L) and MB (10 mg/L) to the tune of ~95% and ~98% respectively at agitation speed of 520±20 rpm and pH of 6.8±0.2. The effects of contact time, dose of adsorbent and dye concentration were investigated. Decolorisation of dyes from aqueous media followed adsorption and photodegradation in UV-light. The adsorption process of both dyes followed the pseudo-second order reaction model, whereas, for photodegradation it was arbitrary. The plausible photodegradation mechanism was proposed. The adsorption process follows neither the pore diffusion nor the film diffusion model. Turnover study results suggested the gradual suppression of loading solute dye on TNT surfaces.

Keywords: TNTs, crystal violet, methylene blue, adsorption/photodegradation.

Introduction

The amount of dye wastewater is increasing day by day and these are formed during dyes production process as well as when the dyes are utilized in different processes viz. printing, cosmetics, textile, paper, leather and rubber industries. Industrial dyes effluent constitutes one of the largest classes of organic pollutants. About 7.0×10^5 tons of dyes pollutants are manufactured yearly worldwide. Around 15–20% dyes effluents are discharged to the water bodies leading to severe contamination[1]. The dyes effluents affect the natural growth and functioning of the aquatic flora and fauna. Different methods are being used to eliminate dyes from wastewater. These include photo-degradation, adsorption, electrochemical process, coagulation, filtration, reverse osmosis, and biochemical processes[2–5]. Among these, adsorption/photodegradation method is considered be the most efficient method for removal of dyes. Many researchers show either adsorption kinetics or photodegradation kinetics in their study, but not the both[6–8]. In this novel study we discuss about the kinetics of both the adsorption and photodegradation for both the dye CV and MB removal using hydrothermally synthesized titanate nanotubes.

Materials and methods

Appropriately diluted solutions of analytical reagent grade chemicals were made. Deionized water was used to prepare all aqueous solutions. Stock solutions (500 mg/L) of CV (λ_{max} = 587 nm, $C_{25}N_3H_{30}Cl$) and MB (λ_{max} = 663 nm, $C_{16}N_3H_{18}ClS$) were prepared and diluted as per the necessity. Titanium dioxide (TiO_2, ~99% purity) was purchased from Loba chemicals. The absorption spectra of different diluted solutions were taken using UV-1800 spectrophotometer (Shimadzu, Japan) using 1-cm quartz cell. Shape and size of nanotubes were measured using a TEM (JEM-1400, JEOL, Japan) at 120 kV. FEI-SEM (Apreo LoVac) was used for SEM/EDX study. For stirring purposes, an electronic magnetic stirrer (Remi, 2MLH) was used. The emission of photons on the solutions was done by UV-light source of 360 nm of 18 W

(UV-C, make: Germany). A black cloth was used for the shielding of the set-up in order to avoid the transmission of UV rays to the outside atmosphere (Fig. 1).

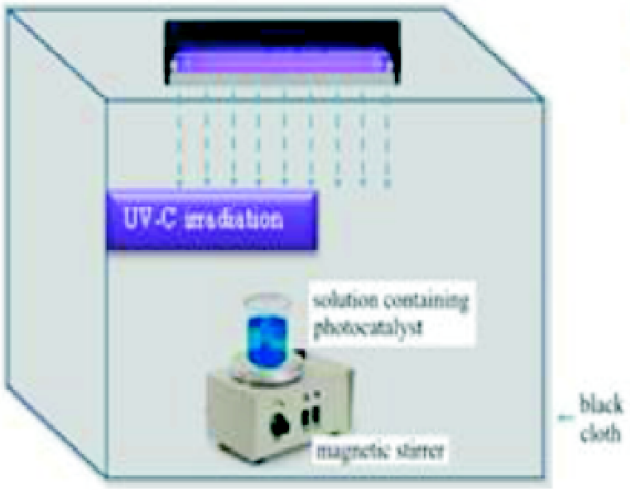

Fig. 1. UV-light set-up for photodegradation.

Previously developed one-step hydrothermal heat treatment method was adopted to synthesize the titanate nanotubes (TNTs) in the laboratory[9]. Firstly, 25 g of TiO_2 powder was added into a 100 mL 10 *M* NaOH solution. The gluey type of suspension was shaken for 1 h using a magnetic stirrer. Next, the suspension was kept into a teflon lined reactor shielded by stainless steel, which was warmed at 150°C for a span of 14 h. Then the suspension was brought down to ambient temperature and washed with deionized water until the pH value reached ~7. Finally, a white solid product was obtained. This solid product was centrifuged at 9000 rpm for a time of 10 min in order to separate TNT. It was then dried at 80°C for continuous 6 h in a hot air oven. The final product was then kept in a black container maintaining dark condition. Characterization of TNT by SEM/EDX and TEM were conducted to understand the surface morphology, size and shape (diameter 50 nm, S_{BET} = 186.8 m^2/g). This TNT was applied to remove CV and MB from aquatic environment in batch mode using adsorption and photodegradation techniques under different experimental conditions to understand the kinetics of adsorption as well as photodegradation on the semiconductor TNTs surfaces.

Adsorption study was carried out at dark condition; however, photo-degradation study was performed in the presence of UV-light (UV-C, 18 W, 360 nm) with the existence of sufficient amount of oxygen in the suspension. Separately, 50 mL of each dye solution was taken in 500 mL beaker (cross-sectional area: 55.44 cm^2). TNTs were added to the dye solutions and the resulting suspensions were agitated in a magnetic stirrer with speed of 520±20 rpm. After achieving the maximum percentage of dye removal (adsorption + photodegradation), suspension was centrifuged (not filtered) at 9000 rpm for 8–9 min. Aliquot of 3 mL was pipetted out to measure the residual dye concentrations spectrophotometrically (UV-1800, Shimazdu, Japan) of each dye in the effluents. Based on the measurement results the standard calibration curves for CV (range: 0–20 mg/L) and MB (range: 0–8 mg/L) were prepared.

Results and discussion

The most promising technique of one-step hydrothermal synthesis method is that the TiO_2 nano particles could turn into a state of exfoliated nano sheets under the hydrothermal reaction in alkaline NaOH solution and rolled to nanotubes[9,10]. The purchased TiO_2 powder upon treatment with alkaline NaOH solution, the positive charge of Na^+ ion get entrapped in between the octahedral layers of $Na_2Ti_3O_7$ and edge-shared of TiO_6. In this condition, a positive static interaction force holds the layer of TiO_6 and Na^+ tightly and disallows the rolling of nanotube. During the hydrothermal treatment, the intercalated Na^+ ions between the TiO_6 sheets will be replaced by H_2O molecules. Larger size of H_2O molecule in comparison to Na^+ aids in widening of interlayer distance during replacement process of Na^+ ions and H_2O molecule. This will reduce the interaction force between the TiO_6 and octahedral layers. The layered $Na_2Ti_3O_7$ particle will then progressively get exfoliated to form several sheet-shaped products and finally rolled to nanotubes[9,10] and is depicted in Fig. 2[9].

The synthesized TNT was characterized by TEM and SEM/EDX study (Fig. 3). As SEM study was not sufficient to detect the actual size and shape of the precursor hence TEM study was performed. TEM image (Fig. 3) clearly suggested the formation of TNT with an average diameter of 50 nm (S_{BET} = 186.8 m^2/g). The sorret band (Fig. 4) of the TNT suggested the occurrence of titanium with additional trace

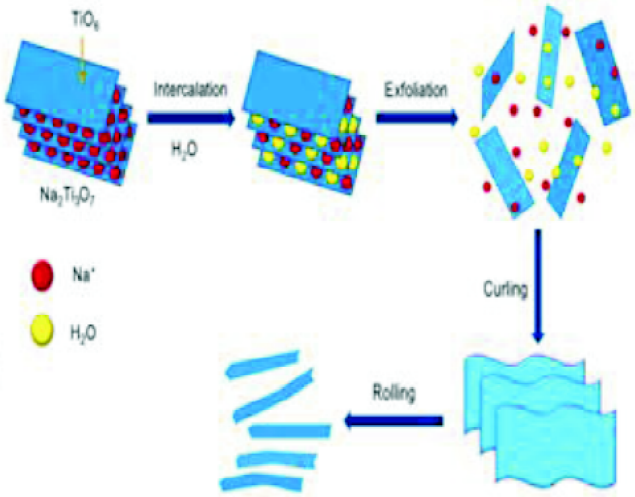

Fig. 2. Schematic diagrams for the synthesis of TNT.

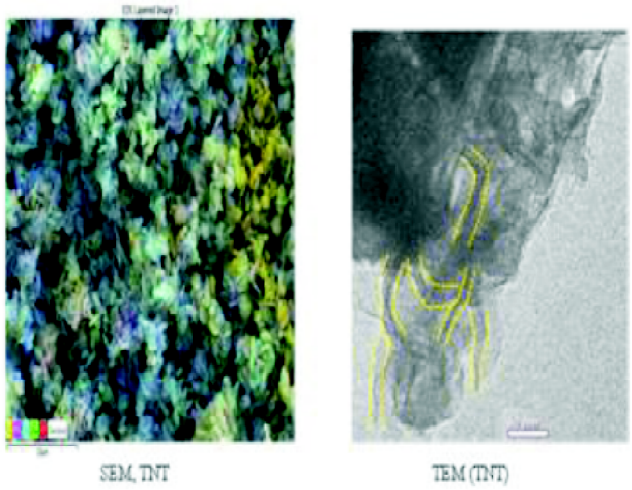

Fig. 3. SEM and TEM of TNT.

impurities as the TiO_2 is only ~99% pure.

Linear equations for CV and MB were Absorbance = 0.095×Concentration (mg/L) + 0.01, the specific relation coefficient R^2 = 0.998 and Absorbance = 0.202×Concentration (mg/L) + 0.0695, the specific correlation of R^2 = 0.997, obtained from standard calibration curve of CV (λ_{max} = 587 nm) and MB (λ_{max} = 663 nm), respectively.

The effect of contact time on decolorisation of both CV and MB dyes by TNTs was performed. The results clearly illustrate that dyes were completely decolorized (removed) after 6 h with over 95% (CV) and 98% (MB) decolorisation.

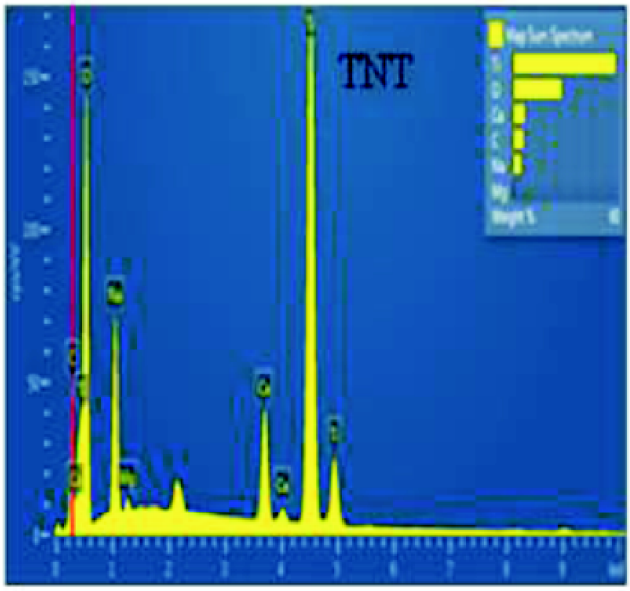

Fig. 4. EDX sorret band of TNT.

The UV-Vis spectrum for the control CV and MB at initial time and for the TNTs mixed dye samples at different time periods are presented in Figs. 5A and 5B. The peaks for CV and MB at initial time were detected at 587 nm and 663 nm respectively. These peaks gradually decreased during the adsorption/degradation without bathochromic or hypsochromic shift in λ_{max}. Both the studies, that is adsorption (in dark) and photodegradation (in UV-light) were conducted for synthetic CV and MB spiked water samples, where the dose of TNT in each case was 3 g/L and the concentrations were 20 mg/L and 10 mg/L, respectively at a pH of 6.8±0.2. The suspensions were taken in a beaker of cross-sectional area 55.44 cm^2 and stirred on a magnetic stirrer at 520–540 rpm at room temperature (25±2°C) in dark for the adsorption process. The obtained result revealed that the maximum adsorption of CV and MB were ~81% and ~85% within the time of 2 h and 1.5 h, respectively (maximum saturation point). The same suspensions were then photo-irradiated (UV-C, 360 nm) and stirred finally to achieve ~95% and ~98% degradation of dyes from aqueous media within the time of 4 h and 4.5 h, respectively. For the photodegradation, the removal percentage of the dyes occurred at a slow rate comparatively than the adsorption rate. Initially the fresh and active sites of TNTs were efficient to adsorb the dyes from the water medium; hence the maximum removal efficiency (%) was achieved. Later

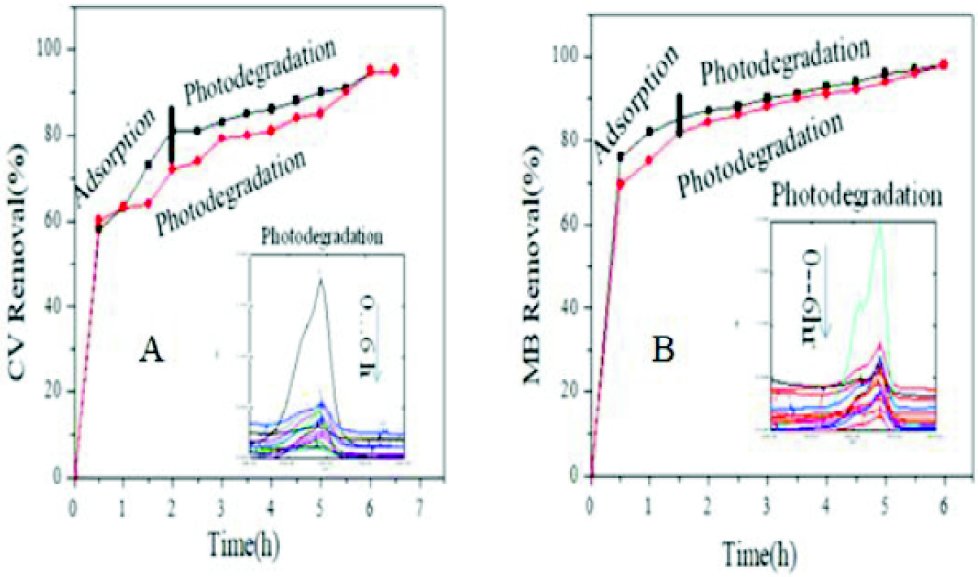

Fig. 5. (A, B) Adsorption and photodegradation of CV and MB synthetic water.

photodegradation process may not have the more active sites for electronic transition from valence band to conduction band to mineralize the solute, dye(s) from the aquatic environment. The kinetics of adsorption and photo-degradation of CV and MB spiked water samples are shown in Figs. 5A and 5B, respectively.

Effect of initial concentrations of dyes were investigated at different concentrations (10–40 mg/L and 5–14 mg/L, for CV and MB spiked water respectively), keeping the other conditions same. The removal efficiency suppressed from ~95% to ~71% for CV synthetic water sample whereas for MB synthetic water sample it was ~98% – 83%, on complete adsorption/photodegradation study. However, 3 g/L dose of the precursor was found to be effective for CV and MB at initial concentrations of 20 mg/L and 10 mg/L, respectively and was designed for further studies. Figs. 6A and 6B show the removal efficiency of CV and MB spiked water with different concentrations.

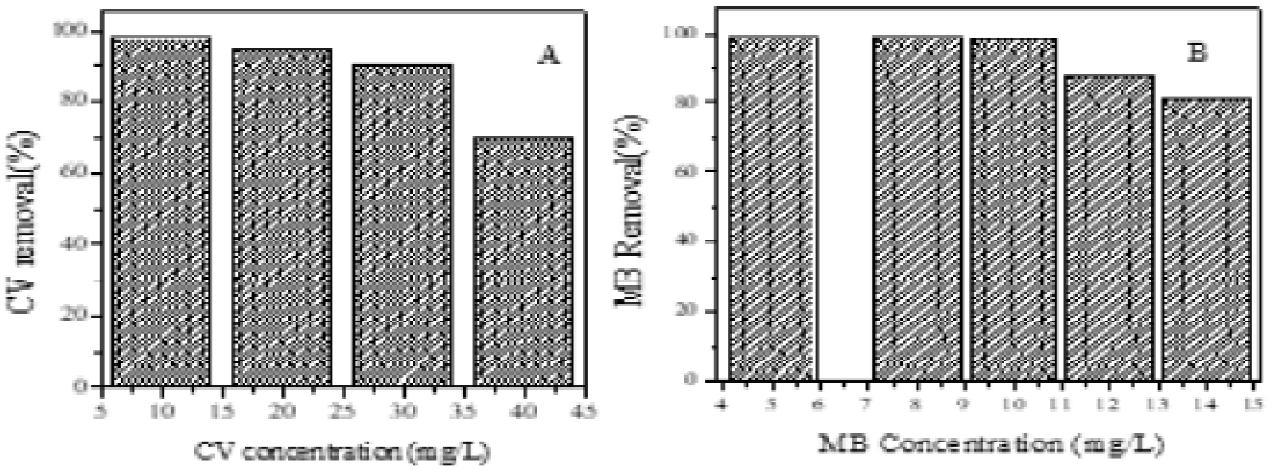

Fig. 6. (A, B) Concentration variation of CV and MB synthetic sample.

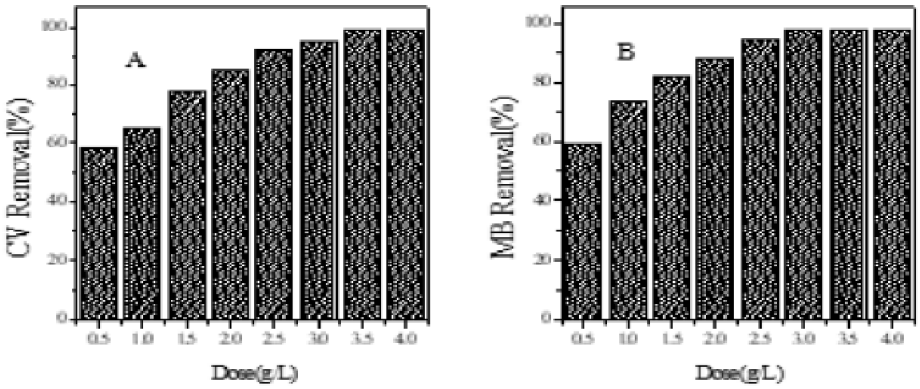

Fig. 7. (A, B) Dose variation of CV and MB synthetic sample.

The efficiency of loading an adsorbent/photocatalyst can be maximized by varying the dose and hence the adsorption/degradation of dyes upon the TNTs as a function of sorbent dose was studied. The effect of dose of TNTs on the degradation of dyes was conducted over a range of 0.5–4 g/L in each case when the other conditions were fixed. As elucidated in Figs. 7A and 7B, the efficiency of dye degradation increased from 58% to 95% for CV and 59% to 98% for MB, when the adsorbent dose increases from 0.5 g/L to 4 g/L. The study was conducted following both the mechanisms of adsorption and photodegradation.

The increment of efficiency of degradation with the variation of dose owed to increase in surface area or may be due to the availability of more precursor active sites. Further by increase in the adsorbent dose beyond the optimum dose, the efficiency become stagnant due to overlapping of sites as a result of overcrowding of precursor with respect to fixed chemical moieties. Hence, the dose 3 g/L was used in each case for the entire studies. Different types of kinetic models were used for the interpretation of the controlling mechanism of the process to corroborate the experimental data[11].

Equation for first-order reaction can be expressed as follows:

$$-\frac{dC_t}{dt} = k_1 C_t \quad (1)$$

After integrating the above equation and at initial conditions we get:

$$\ln C_t = \ln C_0 - k_1 t \quad (2)$$

The variations of $\ln C_t$ with t are presented in Figs. 8A, 9A, correspondingly for CV and MB, respectively.

The pseudo- first order kinetics only describes the sorption sites and not the adsorption process as a whole and can be expressed as:

$$\frac{dq_t}{dt} = ks_1(q_1 - q_2) \quad (3)$$

Integrating the above equation, we get the following expression at initial conditions:

$$\ln (q_1 - q_t) = \ln (q_1) - ks_1 t \quad (4)$$

The plot between $\ln (q_1 - q_t)$ and t yields a straight line. This shows the reaction to be of pseudo-first order (Figs. 8B, 9B, correspondingly for CV and MB).

In adsorption, the concentration of adsorbate follows second order rate equation and can be represented mathematically as:

$$-\frac{dC_t}{dt} = k_1 C_t^2 \quad (5)$$

After integrating the above equation we get at initial conditions in the given form:

$$\frac{1}{C_t} - \frac{1}{C_0} = k_2 t \quad (6)$$

Figs. 8C, 9C represent the variation of $1/C_t$ with t for the dyes CV and MB respectively. The pseudo-second order model, based on the sorption equilibrium capacity, may be expressed as:

$$\frac{dq_t}{dt} = k(q_e - q_t)^2 \quad (7)$$

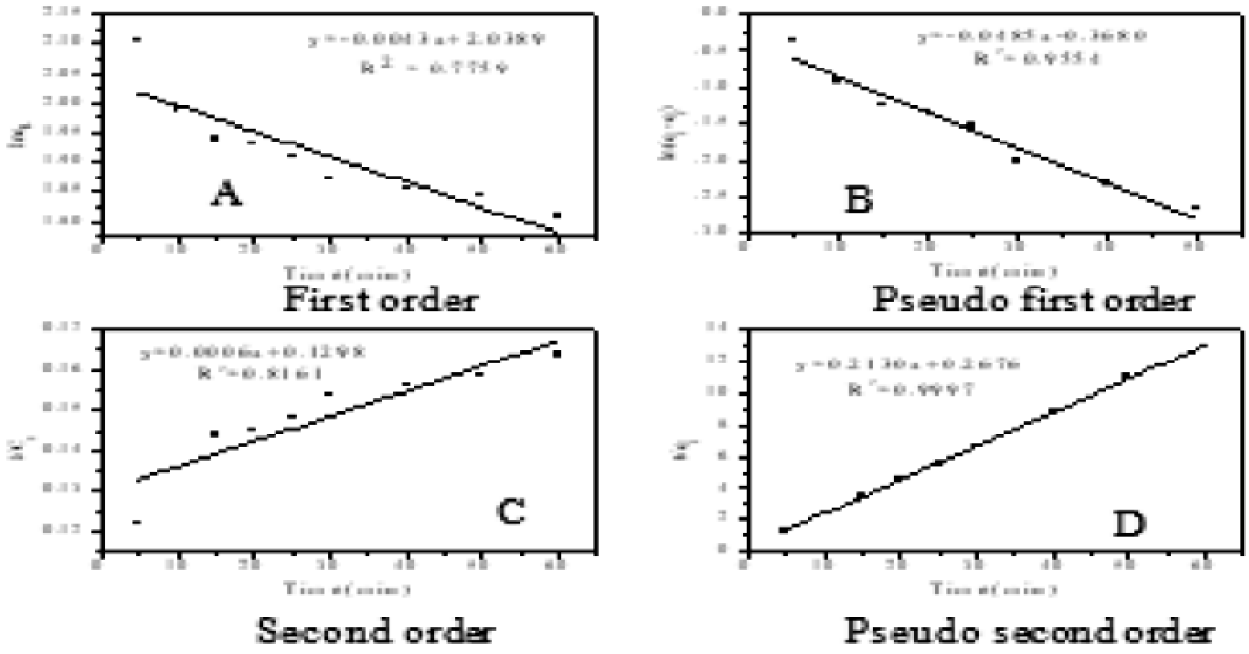

Fig. 8. (A, B, C, D) Adsorption kinetics of CV synthetic sample.

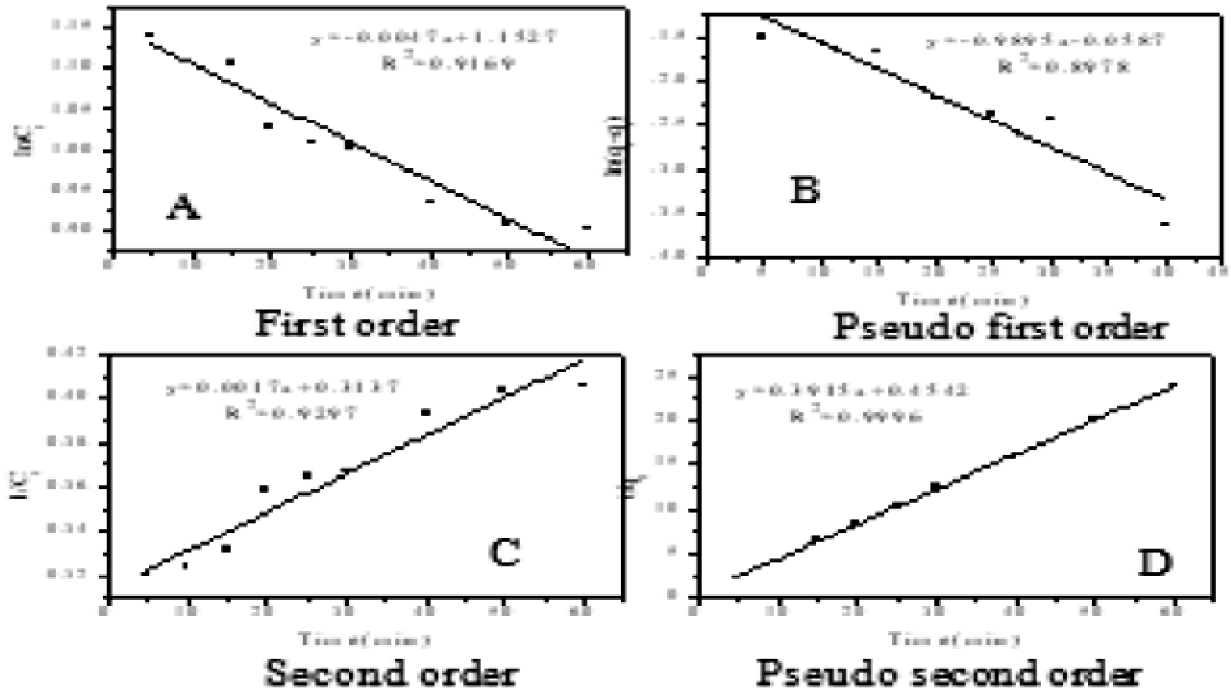

Fig. 9. (A, B, C, D) Adsorption kinetics of MB synthetic sample.

After integrating the above equation, at initial conditions we get:

$$\frac{t}{q_t} = \frac{1}{h} + \frac{1}{q_e}t \quad (8)$$

where $h = kq_e^2$. The plot between t/q_t and t clearly shows linearity and thus can be concluded that the reaction rate follows pseudo-second order kinetics. Figs. 8D, 9D correspondingly for CV and MB spiked synthetic water sample shows the plot for pseudo-second order model.

All the corresponding linear equations with specific relation coefficient values were aggregated in Table 1 and Table 2, correspondingly for CV and MB spiked water sample. It is inferred from the Table 1 and Table 2 that the adsorption of dyes on TNT surfaces followed the pseudo-second-order model best than others. Similarly, the photodegradation mechanism was also evaluated (figure not shown) and the related equations of four models were tabulated in Table 1 and Table 2. The obtained results suggested that the photodegradation of dyes didn't follow sequentially due to photo-adsorption i.e. pseudo-second order reaction model. An arbitrarily reaction model followed by the CV (second order) and MB (first order) spiked water. The photodegradation of dyes on TNT surfaces is due to the transfer of electron(s) from the valence band to the conduction band and is completely different from the adsorption which is a surface phenomenon.

The diffusion coefficients for the intra-particle transport of CV and MB within the pores or films of TNTs were calculated. By utilizing the first order kinetic data, the rate-limiting stage of the adsorption process was evaluated[12]. Considering the spherical morphology of the adsorbent, the pore diffusion coefficient and film diffusion coefficients can be determined using eq. (9) and eq. (10) respectively as follows:

$$t_{1/2} = 0.030\frac{r^2}{D_p} \quad (9)$$

$$t_{1/2} = 0.23\frac{r\delta}{D_f} \times \frac{C_s}{C_e} \quad (10)$$

where, $t_{1/2}$ = time beyond which adsorbate concentration reaches half its initial concentration, r = radius of the adsorbent particle, D_p = pore diffusion coefficient, D_f = film diffusion coefficient, C_s = concentration of the adsorbate on the adsorbent, C_e = concentration of adsorbate in solution at equilibrium, δ = film thickness. The value of $t_{1/2}$ can be determined knowing the value of k_1 (first order reaction rate constant) using the following relationship[12]:

$$t_{1/2} = -\frac{\ln(0.5)}{k_1} \quad (11)$$

The values of D_p and D_f can be estimated then for initial dye

Table 1. Linear equations of four kinetic models of CV spiked water

	CV Synthetic water			
Kinetics	Adsorption kinetics		Photodegradation kinetics	
	Linear equation	R^2	Linear equation	R^1
First order	y = –0.0043x + 2.0389	0.7759	y = –0.2986x + 1.4441	0.9696
Pseudo-first order	y = –0.0485x – 0.3680	0.9554	y = –0.7110x + 0.3552	0.8357
Second order	y = 0.0006x + 0.1298	0.8161	y = –0.6947x + 3.8959	0.9843
Pseudo-second order	y = 0.2130x + 0.2676	0.9997	y = 0.8076x + 1.5072	0.6718

Table 2. Linear equations of four kinetic models of MB spiked water

	MB Synthetic water			
Kinetics	Adsorption kinetics		Photodegradation kinetics	
	Linear equation	R^1	Linear equation	R^2
First order	y = –0.0047x + 1.527	0.9169	y = –0.0056x + 0.4779	0.9661
Pseudo-first order	y = –0.9895x – 0.0587	0.8978	y = 0.0083x – 0.6684	0.9128
Second order	y = 0.0017x + 0.3137	0.9297	y = 0.0078x + 0.4115	0.8484
Pseudo-second order	y = 0.3915x + 0.4542	0.9996	y = 1.8328x + 290.7	0.5619

Table 3. Coefficient values of "film diffusion" and "pore diffusion" for CV and MB spiked water

Initial	C_e (mg/L)	k_1 (l/s)	$t_{1/2}$ (s)	r (cm)	D_f (cm^2/s)	D_p (cm^2/s)
[CV] = 20	~9.45	7.16×10^{-5}	9.7×10^{3}	26×10^{-7}	2.4×10^{-13}	2.09×10^{-17}
[MB] = 10	~5.42	7.83×10^{-5}	8.8×10^{3}	26×10^{-7}	3.85×10^{-13}	2.30×10^{-17}

concentration of 10 mg/L MB and 20 mg/L CV assuming film thickness of (δ) = 0.001 cm and are showed in Table 3. It is well known that if the film diffusion coefficient (D_f) value falls in the array of 10^{-6} to 10^{-8} cm^2/s then film diffusion process would be rate-limiting step and for pore diffusion process the pore diffusion coefficient (D_p) value will reside in the range of 10^{-11} to 10^{-13} cm^2/s. The calculated D_p and D_f, were 2.09×10^{-17}, 2.30×10^{-17} cm^2/s and 2.40×10^{-13}, 3.85×10^{-13} cm^2/s, respectively for CV and MB spiked water sample. In the present study the obtained values suggested that the adsorption of both dyes on TNT surfaces did not follow either of these two. However, the adsorption of dyes in dark may be due to the external diffusion onto the TNT surfaces. Unlike metals or metalloids (ion-exchange) the organic contaminants may behave differently with the sorbent surfaces and hence the results were obtained[12].

The TNT particles gets excited when illuminated with UV-light of energy greater than or equal to its energy band gap ($h\nu \geq E_g$ = 3.2 eV; E_g = band gap energy). This results in the transition of the valency band electron(s) to conduction band and results in the formation of positively charged holes in the valency band. Both the band electron(s) migrate to the oxide surfaces of the sorbent TNT. They react with the chemisorbed O_2 and/or OH^-/H_2O molecules to give $O_2^{\bullet-}$, $HOO^{\bullet}$, and $OH^{\bullet}$ radicals. They react in oxidative degradation by attacking the dye molecules. Else the conduction band electron(s) will react with the dye molecules to form dye radicals anion (Fig. 10). Subsequently radical degrades the dye. The adsorbed dye molecules may be oxidized or reduced by valency band holes to form dye radical cations leading to dye degradation[9,13].

Reusability is essential prerequisite for economic and sustainable application of an adsorbent/photocatalyst. We have recycled the precursor for three cycles by treating with 100% ethyl alcohol and it was observed that even in third cycle, the precursor removed ~69% (CV) and ~46% (MB). Gradual experiments block the active sites of TNT surfaces by the solute molecules hence prohibit the excitation of electron(s) from valence band to conduction band to mineralize the solute molecules. Hence the results obtained.

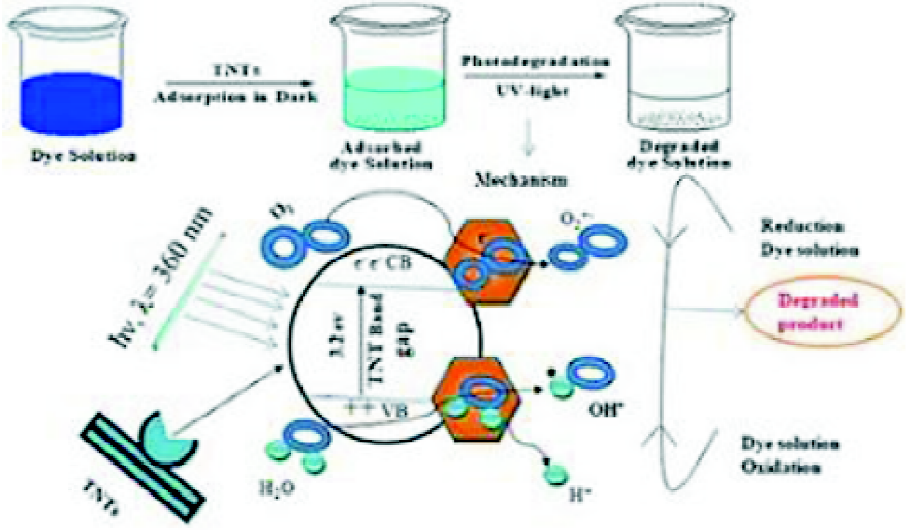

Fig. 10. Probable dye adsorption and photodegradation mechanism.

Conclusion

TNTs were synthesized applying hydrothermal method and successfully utilized to remove CV, MB from aqueous media following adsorption as well as photodegradation. Maximum removals to the tune of ~95% for CV and ~98% for MB from aqueous media were achieved at optimal conditions. Kinetics of the adsorption and photodegradation of both the dye were studied. Pseudo-second order reaction model was followed in case of both the dye adsorption whereas, for photodegradation it was arbitrary. Turnover study for the exhausted precursor was done.

Acknowledgement

The authors acknowledge the financial support received from DST, SERB for the study under the contract number of ECR/2016/001315.

References

1. T. Doy, L. Zang, Y. Zhang, Z. Sun, L. Sun and C. Wang, *Mat. Lett.*, 2019, **244**, 151.
2. M. F. Chowdhury, S. Khandaker, F. Sarker, A. Islam, M. T. Rahman and M. R. Awual, *J. Mol. Liqui*., 2020, **318**, 114061.
3. P. Demircivi and E. B. Simsek, *Wat. Sci. Tech*., 2019, **78**, 487.
4. Y.-L. Ge, Y.-F. Zhang, Y. Yang, S. Xie, Y. Liu, T. Maruyama, Z.-Y. Deng and X. Zhao, *Appl. Surf. Sci.*, 2019, **488**, 813.
5. W. Zhao, X. He, Y. Peng, H. Zhang, D. Sun and X. Wang, *Wat. Sci. Tech*., 2017, **75**, 1494.
6. B. Priyadarshini, T. Patra and T. R. Sahoo, *J. Mag. Allo.,* 2020, in Press.
7. I. Ali, O. M. L. Alharbi, Z. A. Alothman and A. Y. Badjah, *Photochem. Photobio*., 2018, **94**, 935.
8. H. A. Habeeb and A. A. A. Kadhum, *J. Al-Nahrain Univ.*, 2010, **13**, 41.
9. R. Liu, W.-D. Yang, H.-J. Chueng and B.-Q. Ren, *J. Spectro*., 2015, Article ID 680183, 1-9.
10. S. Mohanty, S. Moulick and S. K. Maji, *J. Water Proce. Enging.,* 2020, **37**, 101428.
11. F. Hayeeye, M. Sattar, W. Chinpa and O. Sirichote, *Collo. and Surf. A: Physic. Eng. Asp*., 2017, **513**, 259.
12 S. K. Maji, Y.-H. Kao and C.-W. Liu, *Desali.*, 2011, **280**, 72.
13. M. M. Mahlambi, C. J. Ngila and B. B. Mamba, *J. Nanomat*., 2015, **2015**, 1.